Published in final edited form as:
Mol Cell. 2012 April 13; 46(1): 67–78. doi:10.1016/j.molcel.2012.02.005.

The Glomuvenous Malformation Protein Glomulin Binds Rbx1 and Regulates Cullin RING Ligase-Mediated Turnover of Fbw7

Adriana E. Tron[1,2], **Takehiro Arai**[1,2,§], **David M. Duda**[3,4], **Hiroshi Kuwabara**[1,2,#], **Jennifer L. Olszewski**[3], **Yuko Fujiwara**[5,6], **Brittany N. Bahamon**[7], **Sabina Signoretti**[7], **Brenda A. Schulman**[3,4], and **James A. DeCaprio**[1,2]

[1]Department of Medical Oncology, Dana-Farber Cancer Institute, Boston, MA 02215, USA

[2]Department of Medicine, Brigham and Women's Hospital and Harvard Medical School, Boston, MA 02115, USA

[3]Department of Structural Biology, St. Jude Children's Research Hospital, Memphis, TN 38105, USA

[4]Howard Hughes Medical Institute, St. Jude Children's Research Hospital, Memphis, TN 38105, USA

[5]Division of Hematology/Oncology, Children's Hospital and Harvard Medical School, Boston, MA 02115, USA

[6]Howard Hughes Medical Institute, Harvard Medical School, Boston, MA 02115, USA

[7]Department of Pathology, Brigham and Women's Hospital and Harvard Medical School, Boston, MA 02115, USA

SUMMARY

Fbw7, a substrate receptor for Cul1-RING-ligase (CRL1), facilitates the ubiquitination and degradation of several proteins including Cyclin E and c-Myc. In spite of much effort, the mechanisms underlying Fbw7 regulation are mostly unknown. Here we show that Glomulin (Glmn), a protein found mutated in the vascular disorder Glomuvenous Malformation (GVM), binds directly to the RING domain of Rbx1 and inhibits its E3 ubiquitin ligase activity. Loss of Glmn in a variety of cells, tissues and GVM lesions results in decreased levels of Fbw7 and increased levels of Cyclin E and c-Myc. The increased turnover of Fbw7 is dependent on CRL and proteasome activity indicating that Glmn modulates the E3 activity of $CRL1^{Fbw7}$. These data reveal an unexpected functional connection between Glmn and Rbx1 and demonstrate that defective regulation of Fbw7 levels contributes to GVM.

CONTACT INFORMATION: james_decaprio@dfci.harvard.edu.
[§]Department of Coloproctology, Tokatsu-Tsujinaka Hospital, Chiba, 270-1168, Japan
[#]Department of Surgery, Shuwa General Hospital, Saitama, 344-0035, Japan

The authors declare that they have no competing financial interests.

INTRODUCTION

Mutations in the Glomulin (*GLMN*) gene have been identified in the familial disease Glomuvenous Malformation (GVM, OMIM #13800, Glomus tumors, Glomangioma) (Brouillard et al., 2002; Brouillard et al., 2005). GVMs are cutaneous venous lesions comprised of glomus cells with features of vascular smooth muscle cells (VSMCs) that surround distended vascular lumens (McIntyre et al., 2004). In the hereditary form of GVM, patients inherit a loss-of-function mutant *GLMN* allele followed by a somatic loss of the wild type allele in the affected tissue suggesting growth suppressor functions (Brouillard et al., 2002). However, how Glomulin functions normally and what processes are disrupted in GVM is not understood.

Previously, we identified Glomulin (Glmn, FAP68, FAP48) as a protein associated with the C-terminus of Cul7, a member of the cullin family (Arai et al., 2003). The mammalian cullin family comprises eight members including Cul1, Cul2, Cul3, Cul4A, Cul4B, Cul5, Cul7 and Cul9 (Parc). Cullins are subunits of the Cullin RING Ligase family (CRL) that account for approximately half of the nearly 650 human E3 ubiquitin ligases and almost 20 percent of all cellular proteasome-dependent protein degradation. The C-terminal domain (CTD) of cullins bind to the RING domain proteins Rbx1 or Rbx2 that contribute to recruitment of the E2 ubiquitin conjugating enzyme to the CRL. The N-terminal domain (NTD) of cullin binds to substrate receptors (SR) that recruit the target protein in close proximity to the E2 and facilitate ubiquitin transfer to the substrate.

The E3 ubiquitin ligase activity of CRLs is highly regulated including activation by attachment of Nedd8 to a conserved lysine in the CTD of the cullin (Pan et al., 2004), inhibition by binding to Cand1 (Liu et al., 2002; Zheng et al., 2002a) that interferes with binding of SRs and modification by Nedd8, and deactivation with removal of Nedd8 by the COP9 signalosome complex (CSN) (Lyapina et al., 2001). Notably, the consequences of CSN activity are complex. Removal of Nedd8 by CSN inhibits the E3 ligase activity of CRLs (Cope et al., 2002; Schwechheimer et al., 2001) and reduces the auto-ubiquitination of a subset of SRs *in vivo* resulting in the stable assembly of CRLs (Chew and Hagen, 2007; Cope and Deshaies, 2006; Wee et al., 2005). The specific activity of CRL towards a substrate can be also regulated by post-translational modifications of the SR as well as its corresponding substrates.

Fbw7 (FBXW7, CDC4) is one of the most extensively studied SRs and is a member of the F-box family that together with Skp1 binds to Cul1 to form the $CRL1^{Fbw7}$ complex. Fbw7 has been found to be unstable and regulated by proteasomal degradation (Bashir et al., 2004; Cope and Deshaies, 2006; Wei et al., 2004). A recent study has shown that Fbw7 has a ubiquitin binding domain required for its ubiquitination and turnover (Pashkova et al., 2010). Fbw7 targets substrates containing phosphorylated motifs or phosphodegrons. Among several substrates identified for Fbw7, Cyclin E and c-Myc are the most thoroughly studied (Koepp et al., 2001; Strohmaier et al., 2001; Welcker et al., 2004). Gsk3β-mediated phosphorylation of specific degrons on Cyclin E and c-Myc promotes their binding and degradation by the $CRL1^{Fbw7}$ complex (Welcker et al., 2003; Yada et al., 2004; Ye et al., 2004). Mutation of the Cyclin E and c-Myc phosphodegrons results in loss of binding to Fbw7 and accumulation of these substrates (Minella et al., 2008; Yada et al., 2004). Conversely, mutations in the *Fbw7* gene that disrupt binding to Cyclin E have been detected in many types of human malignancies and result in increased levels of Cyclin E (Akhoondi et al., 2007; Hubalek et al., 2004).

In this study, we demonstrate that Glmn binds directly to the Rbx1's RING domain and inhibits the E3 activity of Rbx1 and associated cullins. We further show that Glmn

specifically affects the CRL-dependent degradation of Fbw7 and consequently the turnover of Cyclin E and c-Myc. Our findings uncover an unexpected functional connection between Glmn and the regulation of Fbw7 and reveal that GVM pathogenesis reflects defective $CRL1^{Fbw7}$ activity.

RESULTS

Glmn Forms Specific Complexes with Rbx1 and Cullins

In an earlier study, we identified Glmn as a protein associated with Cul7 (Arai et al., 2003). However, at that time we did not determine if Glmn interacts with other cullins. Therefore, we tested if myc-tagged cullins were capable of binding to Glmn (Fig. 1A). Endogenous Glmn was co-precipitated by Cul1, Cul3 and Cul4A, weakly by Cul2, and not by Cul5. In contrast, Cand1 was co-precipitated by all cullins tested although the relative amount of Cand1 bound to each cullin differed compared to Glmn (Liu et al., 2002; Zheng et al., 2002a). We also detected reciprocal interaction between endogenous Glmn and Rbx1, Cul1 and Cul4A (Fig. 1B). We then asked if Glmn could also bind to the obligate cullin binding partners Rbx1 and Rbx2. We observed that Glmn was co-precipitated by HA-Rbx1 but not by HA-Rbx2 (Fig. 1C). As expected, HA-Rbx1 and HA-Rbx2 co-precipitated their specific cullin partners, Cul1 and Cul5, respectively (Kamura et al., 2004).

Expression constructs for three GVM-derived Glmn mutations with the smallest truncations compared to wild type were tested for binding to Rbx1 and Cul1 (Brouillard et al., 2002). Glmn m-578 (1711delGT) and m-515 (1547C→G) lack the C-terminal 24 and 79 residues, respectively while m-d393 (1179delCAA) has deleted a single residue. Wild type but not any of the three mutated forms of Glmn could bind to endogenous Cul1 and Rbx1 (Fig. 1D). Other commonly inherited mutations in *GLMN* are frameshifts that result in much larger deletions than the mutations tested here (Brouillard et al., 2002; Brouillard et al., 2005). It is reasonable to conclude that most GVM-associated Glmn mutant proteins are unable to bind to Cul1 and Rbx1.

Glmn Binds the Rbx1's RING Domain and Inhibits E3 Ligase Activity

To further characterize the Glmn and Rbx1 interaction, we mapped the regions of Rbx1 required for binding to Glmn. The N-terminal 23 residues of Rbx1 were required for binding to Cul1 but not Glmn (Fig. 2A) (Furukawa et al., 2002). Loss of the N-terminal 41 residues of Rbx1 significantly reduced the association with Glmn while deletion of the C-terminal 14 residues completely disrupted binding to endogenous Glmn suggesting that an intact RING domain was required for Rbx1 binding to Glmn. We generated Rbx chimeric molecules comprised of the N-terminal strand from Rbx1 or Rbx2 and the C-terminal RING domain from the other. Glmn bound to the chimeric protein containing the RING of Rbx1 but not the RING of Rbx2 (Fig.S1A). We then asked if Glmn could bind to an isolated RING domain of Rbx1 ($Rbx1^{RING}$, residues 36–108). Glmn containing a His_6-MBP-N-terminal fusion co-purified with GST-$Rbx1^{RING}$ in a glutathione-affinity pulldown (Fig. S1B). After removal of the His_6-MBP and GST tags by cleavage with TEV protease, the Glmn-$Rbx1^{RING}$ complex remained intact during gel filtration chromatography (Fig. 2B).

Neddylation of cullins is associated with major conformational changes in the cullin and RING subunits (Duda et al., 2008). We tested if Glmn binding to Rbx1 and Cul1 was affected by neddylation by depleting Cand1, Ubc12 or Csn5, the active subunit of CSN, by siRNA. Knockdown of Ubc12 led to reduction in the amount of neddylated Cul1 and Glmn co-precipitated the predominantly unmodified form of Cul1 (Fig. 2C). Conversely, Csn5 depletion led to a relative increase in neddylated Cul1 that was co-precipitated by Glmn. Depletion of Cand1 had no effect on the levels of neddylated Cul1 or on Glmn binding to Cul1. In addition, Glmn could bind to neddylation-defective cullins (Fig. S1C). We tested if

Glmn could bind to neddylated and un-neddylated Cul1 *in vitro.* Purified, bacterially-produced Cul1-Rbx1 complex (Zheng et al., 2002b) was modified by Nedd8 *in vitro* and incubated with 1 or 5 molar excess of Glmn. Using antibodies against Glmn or Cul1, we detected reciprocal interaction between Glmn and unmodified or neddylated Cul1-Rbx1 (Fig. S1D and E).

To address if Glmn could bind to a fully assembled CRL, we performed gel filtration chromatography assays with purified Glmn and Cul1-Rbx1 or a fully assembled $CRL1^{Fbw7}$ comprised of Cul1, Rbx1, Skp1 and Fbw7ΔD that lacks the dimerization (D) domain of Fbw7 (Hao et al., 2007). Fig. 2D shows co-elution of Glmn with Cul1-Rbx1 and the $CRL1^{Fbw7}$ complex. Together, these results indicate that Glmn can bind to Rbx1-Cul1 and this interaction is not affected by the presence of Skp1-Fbw7.

Rbx1 has multiple E3 functions. First, Rbx1 is an E3 for Nedd8 ligation to cullins. Following neddylation, Rbx1 serves as the E3 ubiquitin ligase in CRL-mediated polyubiquitination of substrates. Since Glmn binds directly to Rbx1's RING domain, we tested if Glmn had any effect on these E3 activities. We observed that Glmn inhibited neddylation of Cul1 using an *in vitro* system (Fig. S1F). We then tested the effect of Glmn on the ubiquitin E3 activity of purified $CRL1^{Fbw7}$ toward a Cyclin E phosphopeptide (Hao et al., 2007). While the $CRL1^{Fbw7}$ complex efficiently promoted the ubiquitination of the phospho-Cyclin E peptide, this reaction was inhibited by addition of Glmn (Fig. 2E).

Given the ability of Glmn to inhibit the E3 activity of a purified CRL *in vitro*, we tested if Glmn could inhibit the ubiquitination activity of a Cul1-Rbx1 complex obtained from human cells. Lysates were prepared from HEK293T cells co-transfected with Flag-Glmn and HA-Rbx1 expression vectors followed by immunoprecipitation with Flag antibody. Flag-Glmn was eluted with Flag peptide and the eluate was re-immunoprecipitated with Rbx1 antibody and subjected to an *in vitro* ubiquitination reaction. As shown in Fig. 2F, Rbx1 bound to Glmn had reduced ubiquitination activity compared to the activity of a similar amount of Rbx1 directly immunoprecipitated from cell extracts. In a similar manner, we tested the ability of Glmn to affect the E3 ligase activity of Cul1. We observed that HA-Cul1 bound to Glmn had significantly reduced ubiquitination activity compared to HA-Cul1 directly immunoprecipitated with HA antibody (Fig. 2G). Together, these results indicate that Glmn can inhibit the E3 ligase activity of Rbx1 and CRL1 complexes.

Glmn-Knockout Mouse Embryos Have Severe Developmental Defects

To gain insight into physiological roles of Glmn, *Glmn*-null mice were generated by the gene-trap method (Zambrowicz et al., 1998). $Glmn^{+/-}$ mice were healthy, fertile and free of any visible skin lesions or tumors over the course of two years. In contrast, no *Glmn*-null offspring resulting from $Glmn^{+/-}$ intercrosses were found at weaning, although $Glmn^{-/-}$ embryos at E7.5–E10.5 were recovered at the expected Mendelian ratio (Fig. 3A). The majority of $Glmn^{-/-}$ embryos died between E10.5 and E12.5 and all homozygote tissues were completely resorbed by E12.5.

Examination of $Glmn^{-/-}$ embryos at E9.5 revealed severe developmental defects. Dysmorphic features included decreased growth, delayed neural tube closure, incomplete axial turning, pericardial effusion and blood cell accumulation in the head and trunk region (Fig. 3B). Although the hearts of $Glmn^{-/-}$ E9.5 embryos were beating regularly when examined, the yolk sac of $Glmn^{-/-}$ embryos failed to form an organized vascular network and blood cells moved slowly within these vessels (Fig. 3C). PECAM-1 staining of whole-mount $Glmn^{-/-}$ yolk sacs revealed a honeycomb-like vascular plexus, indicating an impaired vascular remodeling process (Fig. 3D). The Hematoxylin and Eosin (H&E) stained sections of the head region of E9.5 $Glmn^{-/-}$ embryos showed cystic degeneration and reduced

cellularity of the cephalic mesenchyme (Fig. 3E). Caspase-3 staining revealed that some neuroepithelial and mesenchymal cells were apoptotic (Fig. 3F).

Loss of Glmn Decreases Rbx1 and Cullin Levels and Increases the Abundance of Cyclin E

Given that Glmn binds to Rbx1 and cullins and inhibits Rbx1 E3 activities, we wondered if loss of Glmn had any affect on Rbx1 and cullin levels. Lysates from *Glmn* wild type, heterozygote and null E10.5 viable embryos were western blotted. The levels of Rbx1, Cul1, Cul2, Cul3 and Cul4A proteins were markedly reduced in $Glmn^{-/-}$ embryos (Fig. 4A). Glmn and Rbx1 levels were also slightly reduced in $Glmn^{+/-}$ embryos. In contrast, the levels of Rbx2 and Cul5 in $Glmn^{-/-}$ embryos were comparable to that observed in $Glmn^{+/+}$ or $Glmn^{+/-}$ embryos. Similar results were observed with lysates from E8.5 and E9.5 embryos (Fig. S2A and B).

To exclude the possibility that loss of *Glmn* affected the corresponding mRNA levels, we performed RT-qPCR on RNA prepared from E9.5 embryos. As expected, *Glmn* mRNA levels were diminished in $Glmn^{-/-}$ embryos. However, no changes in *Rbx1, Cul1, Cul2, Cul3* and *Cul5* mRNA levels were observed in $Glmn^{-/-}$ embryos relative to $Glmn^{+/+}$ or $Glmn^{+/-}$ littermates (Fig. 4B). Although *Cul4A* mRNA levels were slightly increased in *Glmn*-null embryos, Cul4A protein levels were markedly decreased relative to $Glmn^{+/+}$ and $Glmn^{+/-}$ embryos (Fig. 4B and A).

Since knockout of *Glmn* had striking effects on Rbx1 and cullin levels, we asked if loss of Glmn could also affect the levels of CRL substrates. We found that although several CRL substrates tested revealed no obvious changes in $Glmn^{-/-}$ embryos compared to wild type and heterozygote (Fig. S2C), Cyclin E and c-Myc levels were increased in $Glmn^{-/-}$ embryo lysates (Fig. 4A). Immunostaining for Cyclin E revealed increased levels in trophoblast giant cells from $Glmn^{-/-}$ placenta relative to $Glmn^{+/+}$ littermate controls (Fig. 4C). In addition, the levels of Rbx1 and cullins were decreased and Cyclin E was increased in lysates prepared from teratomas generated from three independently derived $Glmn^{-/-}$ ES cells compared to wild type cells (Fig. S2D).

We next examined the effect of siRNA knockdown of *Glmn* on the levels of Rbx1, cullins and CRL substrates. Consistent with the results obtained from *Glmn*-knockout mice, loss of *Glmn* led to decreased levels of Rbx1, Cul1 and Cul2, increased levels of Cyclin E and c-Myc while Cul5 levels were unaffected (Fig. 4D). Depletion of Rbx1, expected to disrupt CRL assembly and activity, also resulted in increased levels of Cyclin E and c-Myc while the level of the non-CRL substrate p53 was unaffected. As previously reported, the levels of Cul1 and Cul2 but not Cul5 were reduced in Rbx1 depleted cells (Fig. 4D and (Huang et al., 2009). Other CRL substrates tested revealed no obvious changes after depletion of Rbx1 or Glmn (Fig. S2E).

We made several unsuccessful attempts to generate MEFs from E9.5 $Glmn^{-/-}$ embryos. This effect was likely inherent to the $Glmn^{-/-}$ phenotype since the $Glmn^{+/+}$ and $Glmn^{+/-}$ MEFs were successfully cultured under similar conditions. Alternatively, we were able to generate $Glmn^{-/-}$ ES cells. Stable expression of wild type Glmn but not a GVM-derived mutant (m-d393) or empty vector (EV) in $Glmn^{-/-}$ ES cells increased the levels of Rbx1 and cullins, and reduced the levels of Cyclin E in *Glmn*-null ES cells (Fig. 4E). These results confirm that the effect of the *Glmn*-knockout on the levels of Rbx1, cullins and Cyclin E was due to *Glmn* loss since wild type Glmn but not a GVM mutant form could rescue these effects.

The Reduced Stability of Fbw7 in Glmn Deficient Cells and Tissues Causes Accumulation of Cyclin E and c-Myc

Cyclin E and c-Myc are targeted for ubiquitination and degradation by the $CRL1^{Fbw7}$ complex (Koepp et al., 2001; Strohmaier et al., 2001; Yada et al., 2004). To explore the basis for Cyclin E and c-Myc accumulation in *Glmn* knockout and knockdown cells, we examined Fbw7 levels. We found that Fbw7 levels were decreased in $Glmn^{-/-}$ embryos compared to $Glmn^{+/+}$ and $Glmn^{+/-}$ littermates (Fig. 5A). In addition, we observed a decrease in Fbw7 levels when *Glmn* was depleted from cells by siRNA (Fig. 5B). We did not detect consistent changes in the levels of other SRs or Skp1 in *Glmn* knockdown or knockout cells (Fig. S3A and B).

Phosphorylation of Cyclin E at threonine 380 and c-Myc at threonine 58 by Gsk3β is required for Fbw7 to target these proteins for degradation. As expected, depletion of Fbw7 led to increased levels of Cyclin $E^{pThr380}$ and c-Myc^{pThr58} (Fig. 5B). Interestingly, depletion of *Glmn* also resulted in increased levels of Cyclin $E^{pThr380}$ and c-Myc^{pThr58}. Notably, Gsk3β levels and Cyclin E binding to Cdk2 were unaffected by depletion of *Glmn* or *Fbw7* (Fig. 5B and S3C). Although Cyclin E and c-Myc were appropriately phosphorylated and thereby primed for binding and degradation by the $CRL1^{Fbw7}$ complex, their levels were increased in the absence of Glmn.

Given the accumulation of Cyclin E and decreased levels of Fbw7 in *Glmn*-depleted cells, we examined if there were alterations in their stability. Indeed, the half-life of endogenous Fbw7 was shortened to 11 hours in cells depleted of *Glmn* compared to more than 18 hours in control cells. In contrast, the half-life of total Cyclin E was increased from 6 hours in control cells to 8 hours in *Glmn*-depleted and *Glmn*-null cells (Fig. 5C and S3D). Furthermore, the half-life of Cyclin $E^{pThr380}$ was markedly extended from less than 4 hours in control cells to more than 18 hours in cells depleted of *Glmn* (Fig. 5C). Notably, overexpression of Fbw7 in *Glmn* depleted cells reduced the levels of Cyclin E indicating that Cyclin E levels remained dependent on Fbw7 (Fig. 5D). Furthermore, co-expression of Fbw7 with Gsk3β further reduced levels of Cyclin E in *Glmn* depleted cells. These results indicated that the increased levels of Cyclin E in *Glmn* deficient cells was due, at least in part, to decreased levels of Fbw7.

Since GVM-mutants Glmn failed to bind Rbx1 and were unable to restore the levels of Rbx1, cullins and Cyclin E when overexpressed in *Glmn*-null cells, we wondered if GVM lesions had increased levels of Cyclin E. The levels of these factors were assessed by immunohistochemistry in several unique cases of GVM. Consistent with previous reports, glomus cells within GVM lesions exhibited rounded nuclei, eosinophilic cytoplasm and strong staining for smooth muscle α-actin (Fig. 5E and (McIntyre et al., 2004)). Notably, Cyclin E was detected in a larger fraction of glomus cells compared to normal VSMCs. Quantification of staining revealed that nearly 15% of glomus cells were positive for Cyclin E compared to less than 1% in the corresponding normal VSMCs (Fig. 5F). In addition, c-Myc was detected in more than 90% of glomus cells compared to almost undetectable levels in their normal counterpart (Fig. 5G and H). In contrast, Cul1 and Rbx1 were detected in a smaller fraction of glomus cells compared to normal VSMCs (Fig. 5I–L) in every GVM lesion analyzed.

Together, our data indicates that Glmn loss affects the levels of Cyclin E and c-Myc by modulation of Fbw7 stability. It also suggests that impaired degradation of these two major Fbw7 substrates may contribute, at least in part, to GVM pathogenesis.

Glmn Regulates Rbx1-Directed Ubiquitin-Mediated Proteolysis of Fbw7

Fbw7 has been shown to be unstable and regulated through proteasome-mediated degradation (Bashir et al., 2004; Pashkova et al., 2010; Wei et al., 2004). Therefore, we tested if proteasome inhibition affects the levels of Fbw7 in *Glmn* depleted cells. Indeed, the levels of endogenous Fbw7 in *Glmn* depleted cells were increased when treated with the proteasome inhibitor Bortezomib (Fig. 6A).

A recent report demonstrated that Fbw7 contains an ubiquitin binding domain that promotes its ubiquitination and subsequent turnover (Pashkova et al., 2010). Therefore, we tested if the protein stability of Fbw7, mutated in the ubiquitin binding domain, was affected by depletion of *Glmn*. The half-life of wild type HA-Fbw7 was reduced from more than 6 hours in control cells to 3 hours in *Glmn* depleted cells. In contrast, Fbw7 mutations that diminished ubiquitin binding (Y545A, L583S and D560S, D600S) showed no sensitivity to *Glmn* loss (Fig. 6B–D). Together, these results indicate that *Glmn* loss deregulates the ubiquitin-dependent, proteasome-mediated, turnover of Fbw7.

Previous studies suggested that auto-ubiquitination of F-box proteins within CRL complexes underlies their turnover (Chew et al., 2007; Cope and Deshaies, 2006; Galan and Peter, 1999; Zhou and Howley, 1998). We found that inhibition of the CRL activity with the Nedd8 E1 inhibitor MLN4924 led to increased Fbw7 levels in *Glmn* depleted cells (Fig. 6E). Consistent with this result, reduced CRL activity by siRNA depletion of Rbx1 restored Fbw7 levels in the absence of *Glmn* (Fig. 6F). Notably, gel filtration chromatography assays performed using purified Fbw7 and Glmn revealed no direct association between Glmn and Fbw7 (Fig. S4). These results support the concept that the E3 activity of CRL complexes is required for the increased turnover of Fbw7 in *Glmn* deficient cells.

Glmn Controls the Stability of Rbx1 and Cullin Proteins

Since Rbx1 levels are significantly reduced in *Glmn* deficient cells and GVM lesions (Fig. 4 and 5), we tested if there was alteration in its protein stability. Indeed, the half-life of endogenous Rbx1 was shortened from more than 100 hours in control cells to 12.6 hours, almost 10-fold less, in *Glmn* depleted cells (Fig. 7A and B). Notably, the half-life of Rbx1 was also reduced in $Glmn^{-/-}$ ES cells compared to that in $Glmn^{+/+}$ ES cells (Fig. S5A).

Given the striking effect of *Glmn* loss on the levels of Rbx1 and Rbx1-associated cullins, we asked if this effect was dependent on CRL activity. Blocking de-neddylation by depletion of Csn5 led to an increase in the proportion of neddylated Cul1 and Cul2 compared to the un-neddylated forms and also a reduction in their overall levels (Fig. 7C). Combined depletion of *Glmn* and *Csn5* led to further decreases in Cul1 and Cul2 levels compared to *Glmn* or *Csn5* knockdown alone. In contrast, loss of Ubc12 led to a decrease in the neddylated form of Cul1 and Cul2 and an increase in Rbx1, Cul1 and Cul2 levels. The effects of combined depletion of *Ubc12* and *Glmn* were similar to Ubc12 knockdown alone (Fig. 7C). These results indicate that reduced levels of Rbx1 and cullins in *Glmn* depleted cells were dependent on CRL activity. Consistent with these findings, inhibition of CRL activity with MLN4924 increased the levels of Cul1 and Cul3 in *Glmn* deficient cells (Fig. S5B). Notably, loss of Cand1 had no effect on Rbx1 or cullin levels while simultaneous knockdown of *Cand1* and *Glmn* were similar to *Glmn* depletion alone (Fig. S5C). Together, our data indicate that CRL activity contributes to the increased turnover of Rbx1 and reduced cullin levels in *Glmn* deficient cells.

DISCUSSION

GVM is a localized cutaneous vascular lesion caused by loss-of-function mutations in the *Glmn* gene (Brouillard et al., 2002; Brouillard et al., 2005). Here we demonstrate that Glmn,

but none of three different disease-associated mutants of Glmn, binds specifically to Rbx1, Rbx1-associated cullins and CRL complexes and inhibits Rbx1 E3 activities. We also demonstrate that loss of *Glmn* results in increased turnover of Fbw7 resulting in significantly reduced steady-state levels of Fbw7 that limits the ability of the $CRL1^{Fbw7}$ complex to promote efficient degradation of its substrates Cyclin E and c-Myc. Increased Cyclin E and c-Myc levels were observed in *Glmn*-knockout and knockdown cell lines, teratomas, mouse embryonic tissues, and GVM lesions consistent with inefficient targeting by Fbw7. We observed that point substitution mutations in the ubiquitin binding domain of Fbw7 extended the half-life of Fbw7 in *Glmn* deficient cells. In line with this data, a recent report indicated that the ubiquitin binding activity of Fbw7 and yeast Cdc4 was required for auto-ubiquitination and turnover of the F-box protein (Pashkova et al., 2010). Taken together, our findings uncovered an unexpected link between Glmn, $CRL1^{Fbw7}$, Cyclin E and c-Myc and suggest that defective Fbw7 homeostasis contributes to the development of GVM.

Our findings indicate that the E3 activity of CRL complexes is required for the increased turnover of Fbw7 in cells depleted of *Glmn*. Recent studies on the dynamics of CRLs using quantitative proteomics revealed an increased fraction of F-box SRs bound to Cul1 inactivated by treatment with the Nedd8 E1 inhibitor MLN4924 (Bennett et al., 2010; Lee et al., 2011). Consistent with these reports, inhibition of CRL activity by depletion of Rbx1 or treatment with MLN4924 increased the levels of Fbw7 in *Glmn* depleted cells.

Since increased Cyclin E abundance leads to genomic instability and cancer, its regulation has been the focus of intensive investigation (Spruck et al., 1999). Cyclin E accumulation is often caused by inactivation of $CRL1^{Fbw7}$ that mediates its ubiquitination and degradation (Koepp et al., 2001; Strohmaier et al., 2001). Indeed, mutations of Fbw7 have been found in several cancers and cancer cell lines that result in increased Cyclin E levels (Hubalek et al., 2004; Moberg et al., 2001; Spruck et al., 1999). Previous studies have reported accumulation of Cyclin E in *Fbw7*-null mice (Koepp et al., 2001; Strohmaier et al., 2001; Tetzlaff et al., 2004). Notably, *Fbw7*-null mice have a phenotype similar to that of *Glmn*-null mice, including an impaired vascular network formation and death around E10.5 (Tetzlaff et al., 2004; Tsunematsu et al., 2004). In contrast, disruption of mouse *Rbx1* caused a more striking phenotype with embryonic lethality at E7.5 (Tan et al., 2009).

Cyclin E binding to Fbw7 and subsequent degradation is dependent on phosphorylation of specific degrons (Welcker et al., 2003; Ye et al., 2004). Mutation of these phosphodegrons, especially pThr380, results in loss of binding to Fbw7 and increased levels of Cyclin E *in vivo* (Minella et al., 2008). Using purified proteins, we observed that Glmn could specifically bind to the $CRL1^{Fbw7}$ complex and inhibit the E3 ligase activity toward a Cyclin E pThr380 phosphopeptide. Therefore, on one level, Glmn can directly inhibit the E3 activity of $CRL1^{Fbw7}$ and loss of *Glmn* would be expected to lead to increased degradation of Cyclin E. Instead, we observed that the stability of total and pThr380 forms of Cyclin E as well as the levels of c-Myc, another major Fbw7 substrate, were markedly increased in *Glmn* deficient cells and tissues. This apparent paradox can be explained, at least in part, by the reduced levels of Fbw7 in Glmn deficient cells since overexpression of Fbw7 led to reduction in the levels of Cyclin E. Therefore loss of the inhibitory activity of Glmn towards CRLs led to increased turnover of Fbw7 rather than of its substrates Cyclin E and c-Myc.

In addition to the effects of *Glmn* loss on Fbw7, Cyclin E and c-Myc, we observed reduced levels of Rbx1 and Rbx1-associated cullins in Glmn deficient cells and tissues as well as in GVM specimens. This effect was due to the specific loss of *Glmn* since reintroduction of wild type but not GVM-mutant Glmn restored Rbx1 and cullin levels in $Glmn^{-/-}$ ES cells. Blocking or increasing CRL activity inhibited or enhanced, respectively, the effect of Glmn

loss on the levels of Rbx1 and cullins indicating that Rbx1 E3 activity is required for reduction of Rbx1 and Cullin levels in the absence of Glmn. This is consistent with Glmn functioning as an inhibitor of Rbx1 and Rbx1-associated cullins with loss of Glmn resulting in deregulation of their activity and turnover. Given that RING domains bind E2s and Glmn binds Rbx1's RING domain, the simplest explanation for the inhibition is that Glmn in some way, by direct competition or by indirect effects on RING conformation, acts to prevent Rbx1's RING E3 function of activating cognate E2s.

Similar to Cand1, Glmn binds to a broad range of CRLs although in a completely different manner. Cand1 associates with un-neddylated cullins not bound to SRs. In contrast, Glmn can bind to cullins independent of their neddylation status or association with SRs. However, the specific role of Cand1 in regulating CRL activity remains largely unknown. Depletion of Cand1 had little effect on the abundance of cullins and Cand1 only associates with a small fraction of un-neddylated cullins (Bennett et al., 2010; Lee et al., 2011). Inhibition of neddylation with MLN4924 led to small increases in the fraction of cullins bound to Cand1 and little changes in cullin binding to SRs (Bennett et al., 2010; Lee et al., 2011). Interestingly, loss of Cand1 function in *C. elegans* results in reduction of specific CRL functions while leaving others unaffected (Bosu et al., 2010). Therefore, although Cand1 can bind to the broad class of unmodified Rbx1-Cullins, its impact on CRL activity is quite limited.

Another example of selective CRL regulation is the mammalian UBA-UBX protein UBXD7. While UBXD7 binds a wide range of ubiquitin ligases in cells, including those containing Cul1, Cul2, Cul3 and Cul4, UBXD7 has only been implicated in the turnover of a single CRL ubiquitination target: the $CRL2^{VHL}$ substrate HIF1α (Alexandru et al., 2008). Further studies will be necessary to understand the role of Glmn in controlling the stability of Rbx1 and CRLs as well as its specific effects on Fbw7.

Our data are consistent with an emerging view that there are numerous discrete pools of CRLs with dedicated specific functions. Consistent with this concept, recent studies showed that the distribution of CRL regulatory proteins is not uniform across the various CRL complexes, suggesting that there are distinct modes of regulation controlling the activity of individual CRLs (Bennett et al., 2010). In keeping with this model, Glmn loss had a very specific effect on Fbw7 stability while leaving other SRs unaffected. It is possible that, *in vivo*, Glmn preferentially binds to and stabilizes SR-free forms of cullins, leaving the pool of SR-modified cullins unaffected in the event of Glmn loss. Our study emphasizes that the complexity of CRL regulation cannot be globally explained by cycles of neddylation and Cand1 binding and highlights the need for further studies to clarify these pathways in more detail. It will be interesting to investigate if there are additional modulators of specific CRLs or if control of the majority of CRLs is functionally redundant.

EXPERIMENTAL PROCEDURES

Plasmids and Protein Purification

Human *Glmn* was PCR-amplified from EST clone 3454182. Glmn mutants mut-578, mut-515, and mut-d393 were generated by PCR mutagenesis using the QuikChange kit (Stratagene).

For bacterial expression, full length Glmn was cloned into a modified pRSF-Duet vector (Novagen) containing Maltose Binding Protein (MBP) in frame with the natural pRSF-Duet hexahistidine tag. The RING domain of Rbx1 (residues 36 to the C-terminus) was cloned into pGEX4T1 (Novagen). All other plasmids have been described previously (Duda et al.,

2008; Furukawa et al., 2002; Huang et al., 2009). Details of protein purification, cell culture, cell lines, and antibodies can be found in the Extended Experimental Procedures.

Millennium Pharmaceuticals Inc provided MLN4924.

In Vitro Ubiquitination Reactions

Polyubiquitination (Fig. 2E) was carried out at room temperature with 200 nM Nedd8-modified SCF^{Fbw7}, 0.5 μM Cdc34B, 50 μM ubiquitin and 5 μM biotin-conjugated Cyclin E phosphopeptide in 30 mM Tris-HCL, 20 mM NaCl, 10 mM $MgCl_2$, 5 mM ATP, pH 7.6. Reactions were initiated by addition of 250 nM UBA1. After incubation, reactions were stopped with SDS sample buffer and analyzed by WB. Details of the *in vitro* ubiquitination and neddylation reactions (Fig. 2F, 2G and S1F) are described in the Extended Experimental Procedures.

RNAi

U-2OS, HeLa, HEK293T or ES cells were transfected with 20 nM siRNA duplexes (Dharmacon/Thermo) using Lipofectamine2000 (Invitrogen). Cells were harvested 72 hr after transfection.

Generation of *Glmn* KO ES Cells and Mouse Strain

Procedures for all animal experiments were approved by the Animal Care and Use Committee at Dana-Farber Cancer Institute and in compliance with national and institutional guidelines. The VICTR 48 Omnibank Vector was inserted in intron 1 of the *Glmn* gene in ES cells (gene trap OST109778, Lexicon Genetics) derived from 129/SvEvBrd strain. Heterozygote $Glmn^{+/Gt(OST109778)Lex}$ ES cells were microinjected into C57BL/6J blastocysts and transferred into pseudo-pregnant foster mothers. Chimeric mice were crossed with C57BL/6J mice for germline transmission of the *Glmn* transgene. $Glmn^{+/+}$ and $Glmn^{-/-}$ ES cells were generated from blastocysts. The protocol for genotyping is described in Extended Experimental Procedures.

Histology and Immunohistochemistry

Embryos and deciduas were fixed overnight in Bouin's fixative (Sigma) and 4% paraformaldehyde, respectively, and embedded in paraffin. Sections were stained with H&E or immunostained with the indicated antibodies.

All analyses of GVM specimens were approved by the Committee on Clinical Investigations at Children's Hospital Boston. Sections of GVM tumors were stained with H&E or immunostained with the indicated antibodies following standard procedures. Positive cells were quantified by Aperio automated image analysis system.

RNA Extraction and RT-qPCR

RNA was extracted from embryos using the RNeasy Mini Kit (Qiagen). cDNA was synthesized using Superscript III First-Strand Synthesis System for RT-PCR (Invitrogen), plus oligo (dT) primers. Expression of mRNA was quantified using real-time PCR performed in duplicate with Brilliant SYBR Green QPCR Master Mix according to the manufacturer's instructions (Stratagene). Ct values were normalized against Hprt-1 RNA. The fold increase of expression of $Glmn^{+/-}$ and $Glmn^{-/-}$ was calculated by 2C–T, where T is normalized $Glmn^{+/-}$ or $Glmn^{-/-}$ embryo Ct, and C is normalized $Glmn^{+/+}$ embryo C_T.

Supplementary Material

Refer to Web version on PubMed Central for supplementary material.

Acknowledgments

We are grateful to Hideaki Tanami for help with generation of ES cells and Wenyi Wei for discussions and critical reading of the manuscript. We thank Roderick Bronson (DF/HCC Rodent Histopathology Core), Xiaoqiu Wu and Rosina Liz (DFCI Center for Molecular Oncologic Pathology) for histological analysis, Harry Kozakewich and John Mulliken (Vascular Anomalies Center, Children's Hospital/Harvard Medical School) for providing GVM specimens and Yue Xiong (University of North Carolina School of Medicine) for providing plasmids. This work was supported in part by fellowships from the Pew Charitable Trust and the International Human Frontier Science Program Organization to A.E.T.; Public Health Service grants RO1CA93804, R01CA63113 and P01CA050661 to J.A.D.; and R01GM069530 and R01GM077053 to B.A.S. B.A.S. is an Investigator of the Howard Hughes Medical Institute.

References

Akhoondi S, Sun D, von der Lehr N, Apostolidou S, Klotz K, Maljukova A, Cepeda D, Fiegl H, Dafou D, Marth C, et al. FBXW7/hCDC4 is a general tumor suppressor in human cancer. Cancer Res. 2007; 67:9006–9012. [PubMed: 17909001]

Alexandru G, Graumann J, Smith GT, Kolawa NJ, Fang R, Deshaies RJ. UBXD7 binds multiple ubiquitin ligases and implicates p97 in HIF1alpha turnover. Cell. 2008; 134:804–816. [PubMed: 18775313]

Arai T, Kasper JS, Skaar JR, Ali SH, Takahashi C, DeCaprio JA. Targeted disruption of p185/Cul7 gene results in abnormal vascular morphogenesis. Proc Natl Acad Sci U S A. 2003; 100:9855–9860. [PubMed: 12904573]

Bashir T, Dorrello NV, Amador V, Guardavaccaro D, Pagano M. Control of the SCF(Skp2-Cks1) ubiquitin ligase by the APC/C(Cdh1) ubiquitin ligase. Nature. 2004; 428:190–193. [PubMed: 15014502]

Bennett EJ, Rush J, Gygi SP, Harper JW. Dynamics of cullin-RING ubiquitin ligase network revealed by systematic quantitative proteomics. Cell. 2010; 143:951–965. [PubMed: 21145461]

Bosu DR, Feng H, Min K, Kim Y, Wallenfang MR, Kipreos ET. C. elegans CAND-1 regulates cullin neddylation, cell proliferation and morphogenesis in specific tissues. Dev Biol. 2010; 346:113–126. [PubMed: 20659444]

Brouillard P, Boon LM, Mulliken JB, Enjolras O, Ghassibe M, Warman ML, Tan OT, Olsen BR, Vikkula M. Mutations in a novel factor, glomulin, are responsible for glomuvenous malformations ("glomangiomas"). Am J Hum Genet. 2002; 70:866–874. [PubMed: 11845407]

Brouillard P, Ghassibe M, Penington A, Boon LM, Dompmartin A, Temple IK, Cordisco M, Adams D, Piette F, Harper JI, et al. Four common glomulin mutations cause two thirds of glomuvenous malformations ("familial glomangiomas"): evidence for a founder effect. J Med Genet. 2005; 42:e13. [PubMed: 15689436]

Chew EH, Hagen T. Substrate-mediated regulation of cullin neddylation. J Biol Chem. 2007; 282:17032–17040. [PubMed: 17439941]

Chew EH, Poobalasingam T, Hawkey CJ, Hagen T. Characterization of cullin-based E3 ubiquitin ligases in intact mammalian cells--evidence for cullin dimerization. Cell Signal. 2007; 19:1071–1080. [PubMed: 17254749]

Cope GA, Deshaies RJ. Targeted silencing of Jab1/Csn5 in human cells downregulates SCF activity through reduction of F-box protein levels. BMC Biochem. 2006; 7:1. [PubMed: 16401342]

Cope GA, Suh GS, Aravind L, Schwarz SE, Zipursky SL, Koonin EV, Deshaies RJ. Role of predicted metalloprotease motif of Jab1/Csn5 in cleavage of Nedd8 from Cul1. Science. 2002; 298:608–611. [PubMed: 12183637]

Duda DM, Borg LA, Scott DC, Hunt HW, Hammel M, Schulman BA. Structural insights into NEDD8 activation of cullin-RING ligases: conformational control of conjugation. Cell. 2008; 134:995–1006. [PubMed: 18805092]

Furukawa M, Ohta T, Xiong Y. Activation of UBC5 ubiquitin-conjugating enzyme by the RING finger of ROC1 and assembly of active ubiquitin ligases by all cullins. J Biol Chem. 2002; 277:15758–15765. [PubMed: 11861641]

Galan JM, Peter M. Ubiquitin-dependent degradation of multiple F-box proteins by an autocatalytic mechanism. Proc Natl Acad Sci U S A. 1999; 96:9124–9129. [PubMed: 10430906]

Hao B, Oehlmann S, Sowa ME, Harper JW, Pavletich NP. Structure of a Fbw7-Skp1-cyclin E complex: multisite-phosphorylated substrate recognition by SCF ubiquitin ligases. Mol Cell. 2007; 26:131–143. [PubMed: 17434132]

Huang DT, Ayrault O, Hunt HW, Taherbhoy AM, Duda DM, Scott DC, Borg LA, Neale G, Murray PJ, Roussel MF, Schulman BA. E2-RING expansion of the NEDD8 cascade confers specificity to cullin modification. Mol Cell. 2009; 33:483–495. [PubMed: 19250909]

Hubalek MM, Widschwendter A, Erdel M, Gschwendtner A, Fiegl HM, Muller HM, Goebel G, Mueller-Holzner E, Marth C, Spruck CH, et al. Cyclin E dysregulation and chromosomal instability in endometrial cancer. Oncogene. 2004; 23:4187–4192. [PubMed: 15048079]

Kamura T, Maenaka K, Kotoshiba S, Matsumoto M, Kohda D, Conaway RC, Conaway JW, Nakayama KI. VHL-box and SOCS-box domains determine binding specificity for Cul2-Rbx1 and Cul5-Rbx2 modules of ubiquitin ligases. Genes Dev. 2004; 18:3055–3065. [PubMed: 15601820]

Koepp DM, Schaefer LK, Ye X, Keyomarsi K, Chu C, Harper JW, Elledge SJ. Phosphorylation-dependent ubiquitination of cyclin E by the SCFFbw7 ubiquitin ligase. Science. 2001; 294:173–177. [PubMed: 11533444]

Lee JE, Sweredoski MJ, Graham RL, Kolawa NJ, Smith GT, Hess S, Deshaies RJ. The Steady-State Repertoire of Human SCF Ubiquitin Ligase Complexes Does Not Require Ongoing Nedd8 Conjugation. Mol Cell Proteomics. 2011; 10:M110 006460.

Liu J, Furukawa M, Matsumoto T, Xiong Y. NEDD8 modification of CUL1 dissociates p120(CAND1), an inhibitor of CUL1-SKP1 binding and SCF ligases. Mol Cell. 2002; 10:1511–1518. [PubMed: 12504025]

Lyapina S, Cope G, Shevchenko A, Serino G, Tsuge T, Zhou C, Wolf DA, Wei N, Shevchenko A, Deshaies RJ. Promotion of NEDD-CUL1 conjugate cleavage by COP9 signalosome. Science. 2001; 292:1382–1385. [PubMed: 11337588]

McIntyre BA, Brouillard P, Aerts V, Gutierrez-Roelens I, Vikkula M. Glomulin is predominantly expressed in vascular smooth muscle cells in the embryonic and adult mouse. Gene Expr Patterns. 2004; 4:351–358. [PubMed: 15053987]

Minella AC, Loeb KR, Knecht A, Welcker M, Varnum-Finney BJ, Bernstein ID, Roberts JM, Clurman BE. Cyclin E phosphorylation regulates cell proliferation in hematopoietic and epithelial lineages in vivo. Genes Dev. 2008; 22:1677–1689. [PubMed: 18559482]

Moberg KH, Bell DW, Wahrer DC, Haber DA, Hariharan IK. Archipelago regulates Cyclin E levels in Drosophila and is mutated in human cancer cell lines. Nature. 2001; 413:311–316. [PubMed: 11565033]

Pan ZQ, Kentsis A, Dias DC, Yamoah K, Wu K. Nedd8 on cullin: building an expressway to protein destruction. Oncogene. 2004; 23:1985–1997. [PubMed: 15021886]

Pashkova N, Gakhar L, Winistorfer SC, Yu L, Ramaswamy S, Piper RC. WD40 repeat propellers define a ubiquitin-binding domain that regulates turnover of F box proteins. Mol Cell. 2010; 40:433–443. [PubMed: 21070969]

Schwechheimer C, Serino G, Callis J, Crosby WL, Lyapina S, Deshaies RJ, Gray WM, Estelle M, Deng XW. Interactions of the COP9 signalosome with the E3 ubiquitin ligase SCFTIRI in mediating auxin response. Science. 2001; 292:1379–1382. [PubMed: 11337587]

Spruck CH, Won KA, Reed SI. Deregulated cyclin E induces chromosome instability. Nature. 1999; 401:297–300. [PubMed: 10499591]

Strohmaier H, Spruck CH, Kaiser P, Won KA, Sangfelt O, Reed SI. Human F-box protein hCdc4 targets cyclin E for proteolysis and is mutated in a breast cancer cell line. Nature. 2001; 413:316–322. [PubMed: 11565034]

Tan M, Davis SW, Saunders TL, Zhu Y, Sun Y. RBX1/ROC1 disruption results in early embryonic lethality due to proliferation failure, partially rescued by simultaneous loss of p27. Proc Natl Acad Sci U S A. 2009; 106:6203–6208. [PubMed: 19325126]

Tetzlaff MT, Yu W, Li M, Zhang P, Finegold M, Mahon K, Harper JW, Schwartz RJ, Elledge SJ. Defective cardiovascular development and elevated cyclin E and Notch proteins in mice lacking the Fbw7 F-box protein. Proc Natl Acad Sci U S A. 2004; 101:3338–3345. [PubMed: 14766969]

Tsunematsu R, Nakayama K, Oike Y, Nishiyama M, Ishida N, Hatakeyama S, Bessho Y, Kageyama R, Suda T, Nakayama KI. Mouse Fbw7/Sel-10/Cdc4 is required for notch degradation during vascular development. J Biol Chem. 2004; 279:9417–9423. [PubMed: 14672936]

Wee S, Geyer RK, Toda T, Wolf DA. CSN facilitates Cullin-RING ubiquitin ligase function by counteracting autocatalytic adapter instability. Nat Cell Biol. 2005; 7:387–391. [PubMed: 15793566]

Wei W, Ayad NG, Wan Y, Zhang GJ, Kirschner MW, Kaelin WG Jr. Degradation of the SCF component Skp2 in cell-cycle phase G1 by the anaphase-promoting complex. Nature. 2004; 428:194–198. [PubMed: 15014503]

Welcker M, Orian A, Grim JE, Eisenman RN, Clurman BE. A nucleolar isoform of the Fbw7 ubiquitin ligase regulates c-Myc and cell size. Curr Biol. 2004; 14:1852–1857. [PubMed: 15498494]

Welcker M, Singer J, Loeb KR, Grim J, Bloecher A, Gurien-West M, Clurman BE, Roberts JM. Multisite phosphorylation by Cdk2 and GSK3 controls cyclin E degradation. Mol Cell. 2003; 12:381–392. [PubMed: 14536078]

Yada M, Hatakeyama S, Kamura T, Nishiyama M, Tsunematsu R, Imaki H, Ishida N, Okumura F, Nakayama K, Nakayama KI. Phosphorylation-dependent degradation of c-Myc is mediated by the F-box protein Fbw7. Embo J. 2004; 23:2116–2125. [PubMed: 15103331]

Ye X, Nalepa G, Welcker M, Kessler BM, Spooner E, Qin J, Elledge SJ, Clurman BE, Harper JW. Recognition of phosphodegron motifs in human cyclin E by the SCF(Fbw7) ubiquitin ligase. J Biol Chem. 2004; 279:50110–50119. [PubMed: 15364936]

Zambrowicz BP, Friedrich GA, Buxton EC, Lilleberg SL, Person C, Sands AT. Disruption and sequence identification of 2,000 genes in mouse embryonic stem cells. Nature. 1998; 392:608–611. [PubMed: 9560157]

Zheng J, Yang X, Harrell JM, Ryzhikov S, Shim EH, Lykke-Andersen K, Wei N, Sun H, Kobayashi R, Zhang H. CAND1 binds to unneddylated CUL1 and regulates the formation of SCF ubiquitin E3 ligase complex. Mol Cell. 2002a; 10:1519–1526. [PubMed: 12504026]

Zheng N, Schulman BA, Song L, Miller JJ, Jeffrey PD, Wang P, Chu C, Koepp DM, Elledge SJ, Pagano M, et al. Structure of the Cul1-Rbx1-Skp1-F boxSkp2 SCF ubiquitin ligase complex. Nature. 2002b; 416:703–709. [PubMed: 11961546]

Zhou P, Howley PM. Ubiquitination and degradation of the substrate recognition subunits of SCF ubiquitin-protein ligases. Mol Cell. 1998; 2:571–580. [PubMed: 9844630]

HIGHLIGHTS

1. Glmn binds the RING domain of Rbx1 and inhibits $CRL1^{Fbw7}$ E3 ligase activity
2. *Glmn*-null mice phenotype partially mirrors that associated with loss of Fbw7
3. GVM Glmn mutants fail to bind Rbx1 leading to deregulation of Fbw7 stability
4. GVM lesions reflect abnormal homeostasis of Fbw7, Cyclin E and c-Myc.

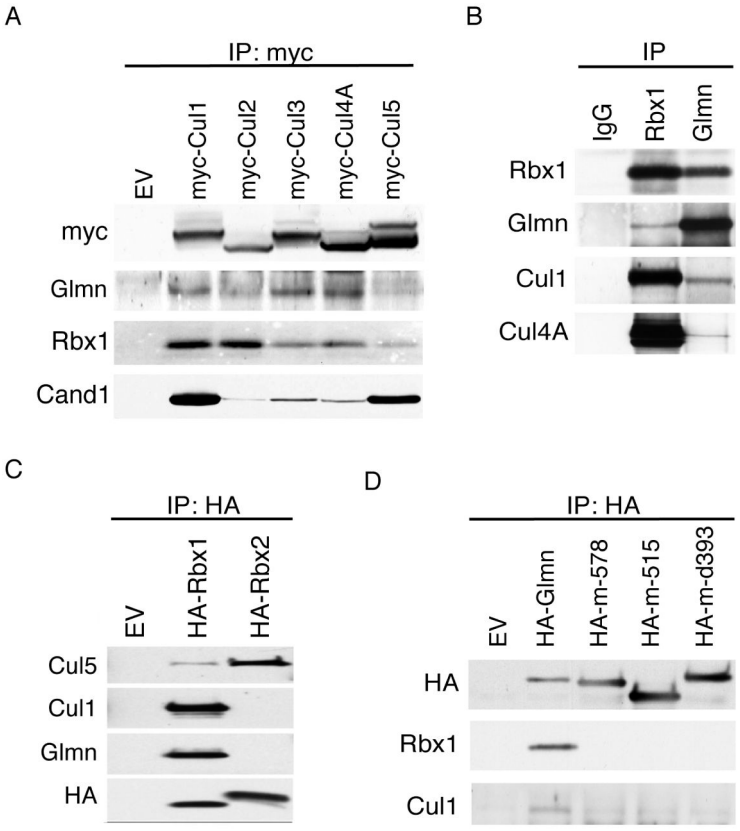

Figure 1. Glmn binds specifically to Rbx1 and Cullins

(**A**) Extracts from HEK293T cells transfected with myc-tagged cullins or empty vector (EV) were immunoprecipitated with Myc antibody and western blotted (WB).

(**B**) U-2OS cell extracts were immunoprecipitated with antibodies against Rbx1, Glmn or control IgG and WB.

(**C**) Lysates of HeLa cells transfected with HA-Rbx1, HA-Rbx2 or EV were immunoprecipitated with HA antibody and WB.

(**D**) Extracts from HEK293T cells transfected with EV, or HA-wild type or -mutant Glmn were immunoprecipitated with HA antibody and WB.

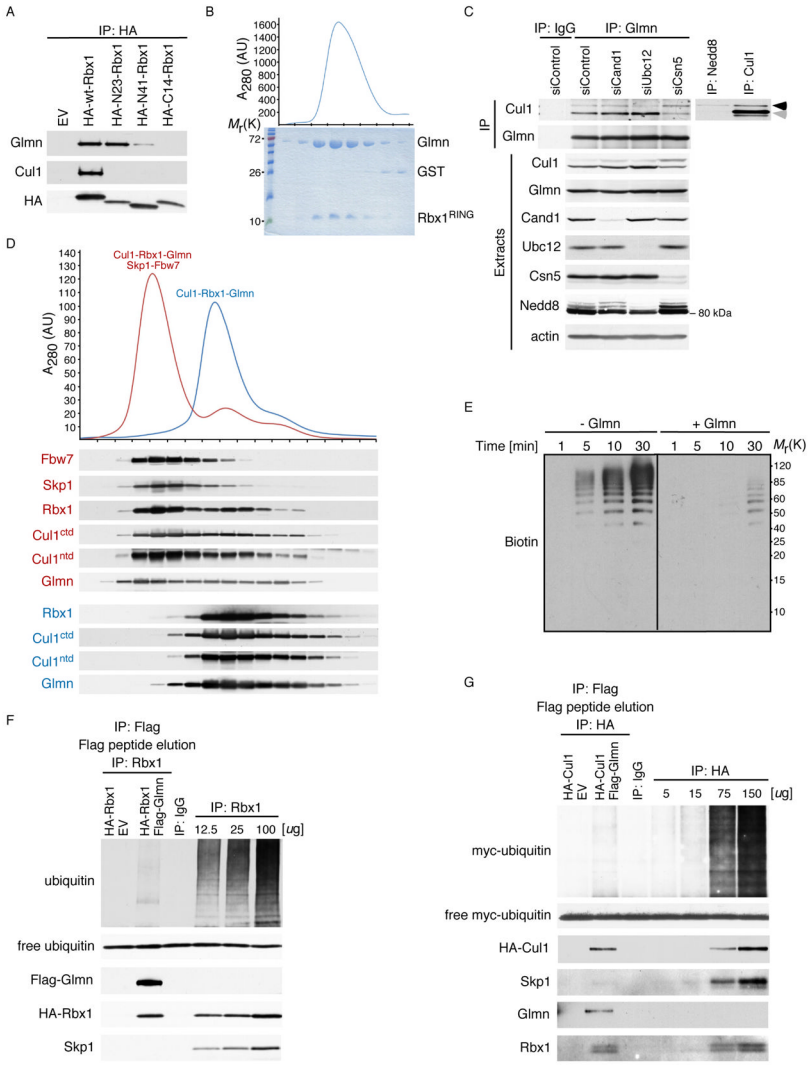

Figure 2. Glmn Binds the RING Domain of Rbx1 and Inhibits E3 Ligase Activity

(**A**) Extracts from HEK293T cells transfected with HA-Rbx1 wild type (wt) or mutants were immunoprecipitated with HA antibody and WB.

(**B**) Upper - Glmn was mixed with purified $Rbx1^{RING}$ and analyzed by gel filtration chromatography. Eluted proteins were detected by spectrophotometry. AU: arbitrary units. Bottom - Coomassie-stained SDS-PAGE gel of the eluted fractions.

(**C**) Lysates from U-2OS cells transfected with the indicated siRNAs were immunoprecipitated and WB. Immunoprecipitation with Nedd8 and Cul1 antibodies were included as controls. Black and gray arrows indicate neddylated and un-neddylated Cul1, respectively.

(**D**) Glmn was mixed with purified Cul1-Rbx1 (blue) or Cul1-Rbx1-Skp1-Fbw7 (red) complexes prior to gel filtration chromatography. Eluted proteins were detected by spectrophotometry (upper panel) and WB (bottom panel).

(**E**) *In vitro* ubiquitination reactions with biotin-labeled Cyclin E phosphopeptide and neddylated $CRL1^{Fbw7}$, in the absence (-, left) or presence (+, right) of Glmn were WB with biotin antibody.

Extracts from HEK293T cells co-transfected with HA-Rbx1 and Flag-Glmn or EV (**F**) or HA-Cul1 and Flag-Glmn or EV (**G**) were immunoprecipitated with Flag antibody. Flag-

Glmn-associated proteins were eluted with Flag peptide, re-immunoprecipitated with Rbx1 (**F**) or HA (**G**) antibody, followed by ubiquitination assay and WB. Increasing amounts of HA-Rbx1 (**F**) or HA-Cul1 (**G**) expressing HEK293T lysates immunoprecipitated with Rbx1 or HA antibody, respectively, and subjected to an ubiquitination reaction were included as positive controls.
See also Figure S1

A

	Glmn genotype				
Age	Total	+/+	+/-	-/-	%-/-
E7.5	29	5	18	6	21
E8.5	40	12	18	10	25
E9.5	52	12	29	11	21
E10.5	40	7	22	11	28
E12.5	46	13	33	0	0
E18.5	11	3	8	0	0
3 weeks	72	31	41	0	0

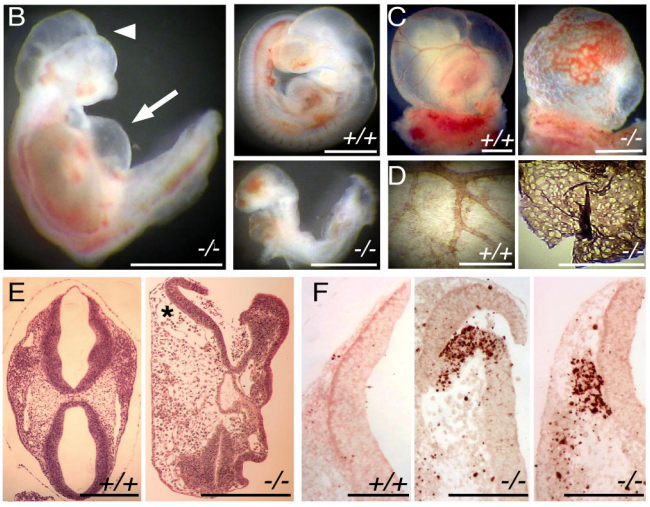

Figure 3. *Glmn*-Null Embryos Have Severe Developmental Defects

(**A**) Genotype of *Glmn*$^{+/-}$ intercrosses. % −/−, Proportion of total *Glmn*$^{-/-}$ embryos or pups at each stage.

(**B**) Gross appearance of *Glmn*$^{-/-}$ E9.5 embryos. *Glmn*$^{-/-}$ embryos showed vast pools of embryonic blood, pericardial effusion (arrow) and asymmetrical open neural tube (arrow head) compared with *Glmn*$^{+/+}$ littermate. Scale bars, 1 mm

(**C**) Yolk sacs of *Glmn*$^{-/-}$ embryos presented disorganized vascular structures. A yolk sac of *Glmn*$^{+/+}$ littermate was included as control. Scale bars, 1 mm

(**D**) *Glmn*$^{-/-}$ E9.5 yolk sacs stained for PECAM-1 showed a primitive vascular plexus compared to wild type control. Scale bars, 0.5 mm

Sections of H&E (**E**) or Caspase-3 (**F**) stained head regions of the *Glmn*$^{-/-}$ E9.5 embryo demonstrated cystic degeneration (asterisk, **E**), low cellularity in mesenchyme (**E**), and massive apoptosis (**F**) compared with *Glmn*$^{+/+}$ littermate. Scale bars, 300 μm (**E**) and 100 μm (**F**)

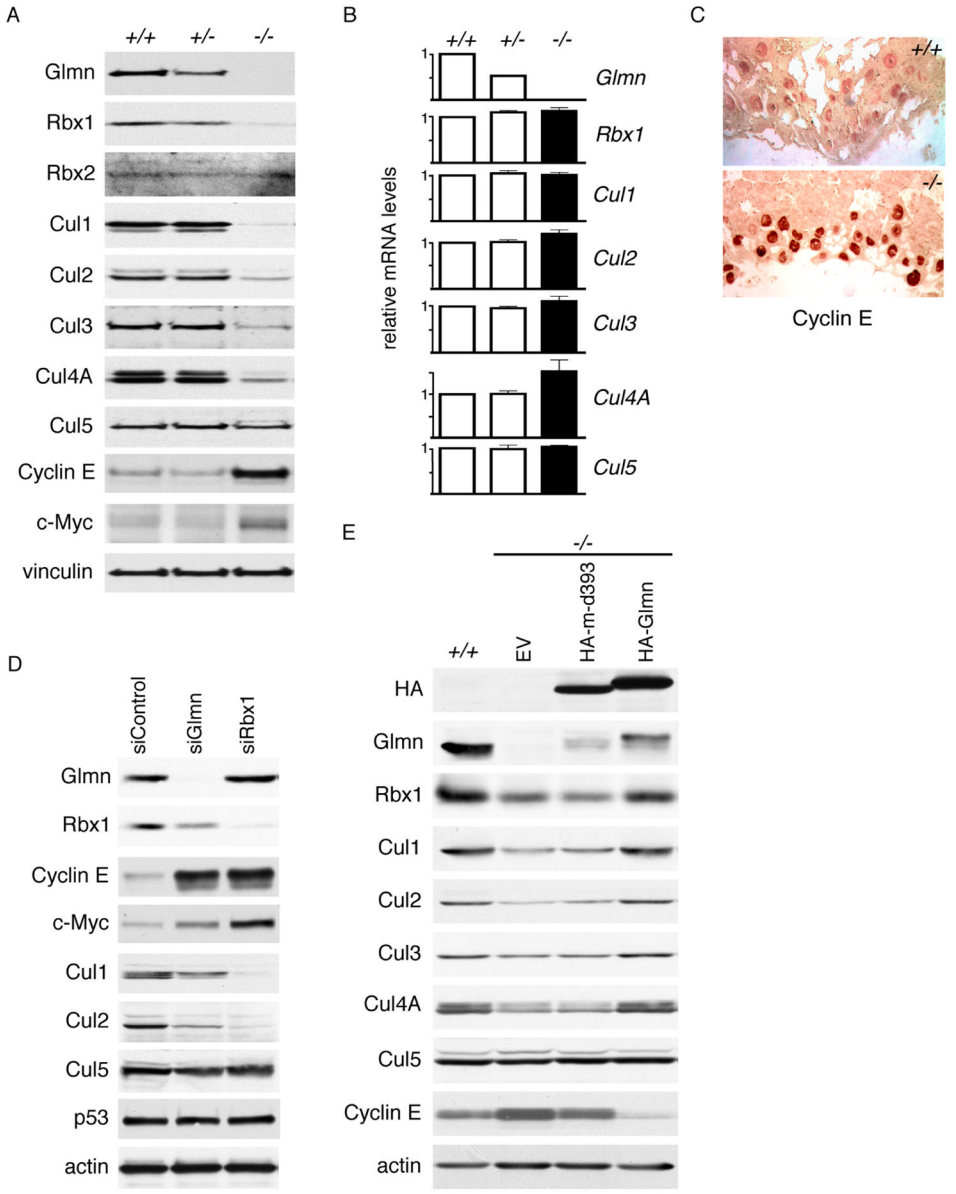

Figure 4. Loss of Glmn Leads to Decreased Levels of Rbx1 and Cullins and Increased Abundance of Cyclin E

(**A**) Lysates from E9.5 *Glmn*$^{+/+}$, *Glmn*$^{+/-}$ and *Glmn*$^{-/-}$ embryo and yolk sac were WB.

(**B**) Relative mRNA levels for indicated genes in *Glmn*$^{+/+}$, *Glmn*$^{+/-}$ and *Glmn*$^{-/-}$ embryos. Results are shown as means ± standard error, calculated from three independent experiments.

(**C**) Sections of *Glmn*$^{+/+}$ and *Glmn*$^{-/-}$ placentas at E9.5 were stained with Cyclin E antibody (200x).

(**D**) Lysates from U-2OS cells transfected with Glmn, Rbx1 or control siRNA were WB.

(**E**) Extracts from *Glmn*$^{+/+}$ or *Glmn*$^{-/-}$ ES cells stably expressing HA-Glmn, HA-m-d393, or EV were WB.

See also Figure S2

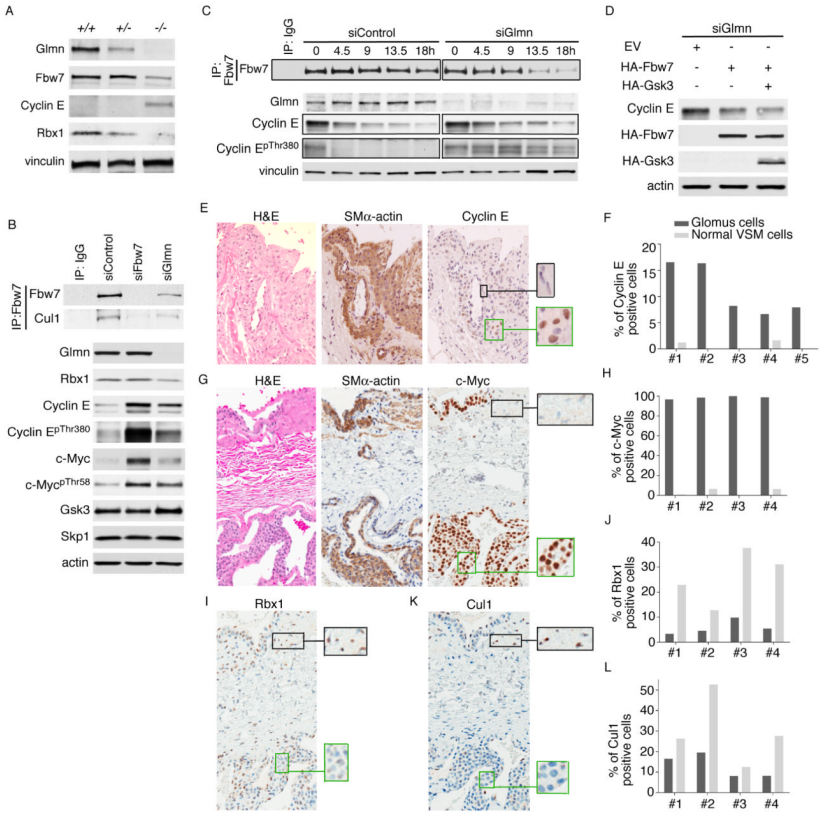

Figure 5. Reduced Stability of Fbw7 in Glmn Depleted Cells Contributes to Cyclin E and c-Myc Accumulation

(**A**) Lysates from E9.5 *Glmn*$^{+/+}$, *Glmn*$^{+/-}$ and *Glmn*$^{-/-}$ embryo and yolk sac were WB.

(**B**) Extracts from U-2OS cells transfected with Glmn, Fbw7 or control siRNA were WB. Fbw7 was immunoprecipitated with Fbw7 antibody followed by WB.

(**C**) Lysates from U-2OS cells transfected with *Glmn* or control siRNA and treated with CHX for the indicated time were WB. To normalize the amount of protein at time zero, blots highlighted in boxes were exposed for different times. Fbw7 was immunoprecipitated with Fbw7 antibody prior to WB.

(**D**) Extracts from U-2OS transfected with *Glmn* siRNA and EV, HA-Fbw7 or HA-Gsk3 plasmids were WB.

Sections of GVM were stained with H&E or immunostained with smooth muscle (SM) α-actin, Cyclin E (**E**), c-Myc (**G**), Rbx1 (**I**) or Cul1 (**K**) antibody. Squares in green outline fields enriched for glomus cells; squares in black shows field with normal VSMCs. Percentage of Cyclin E (**F**), c-Myc (**H**), Rbx1 (**J**), or Cul1 (**L**) positive cells present in sections of different GVM patients was quantified by Aperio analysis.

See also Figure S3

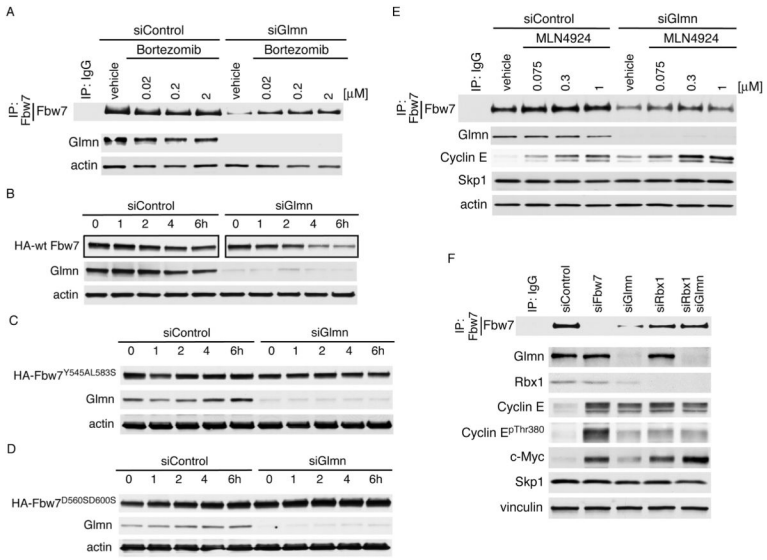

Figure 6. Glmn Inhibits Rbx1-Mediated Ubiquitination of Fbw7

(**A**) Lysates from U-2OS cells transfected with *Glmn* or control siRNA were treated with 0.02, 0.2 or 2 μM Bortezomib for 9 hrs and WB. Fbw7 was immunoprecipitated with an Fbw7 antibody prior to WB.

Extracts from U-2OS cells stably expressing HA-wild type Fbw7 (**B**), HA-Fbw7$^{Y545A,\ L583S}$ (**C**), or HA-Fbw7$^{D560S,\ D600S}$ (**D**) and treated with 100 μg/ml CHX for the indicated time were WB. To normalize the amount of protein at time zero, blots highlighted in boxes were exposed for different times.

(**E**) U-2OS cells transfected with *Glmn* or control siRNA were treated with 0.075, 0.3 or 1 μM MLN4924 for 20 hrs and WB.

(**F**) Extracts from U-2OS cells transfected with the indicated siRNAs were WB.

See also Figure S4

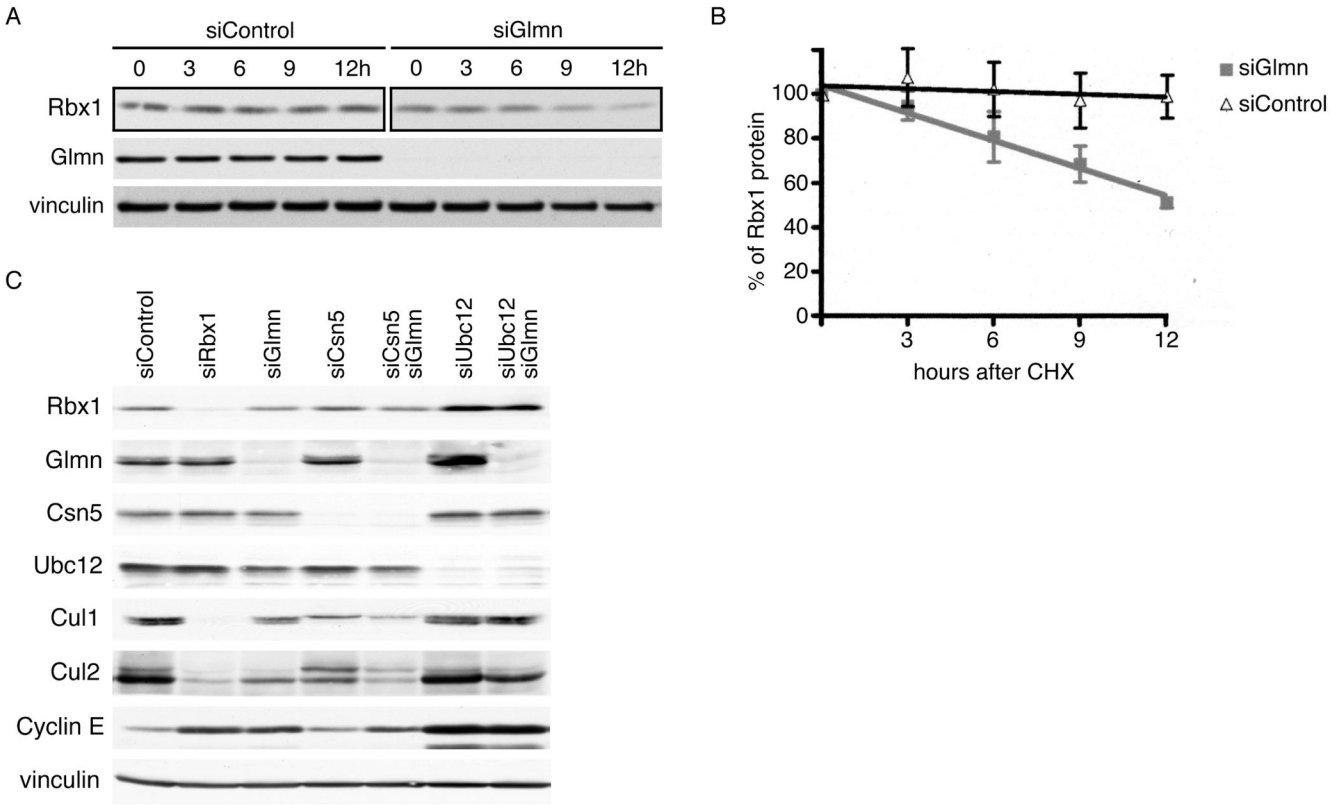

Figure 7. Glmn Controls the Protein Stability of Rbx1 and Cullins

(**A**) Extracts from U-2OS cells transfected with *Glmn* or control siRNA and treated with 50 μg/ml CHX for the indicated time were WB. To normalize the amount of protein at time zero, blots highlighted in boxes were exposed for different times.

(**B**) Graphical representation of Rbx1 abundance in U-2OS cells transfected with *Glmn* or control siRNA after CHX for the indicated times. Data are shown as means ± standard error, calculated from three independent experiments $p < 0.0001$.

(**C**) Lysates from U-2OS cells transfected with the indicated siRNAs were WB.

See also Figure S5